Polymer Vol. 37 No. 7, pp. 1129–1136, 1996
Copyright © 1996 Elsevier Science Ltd
Printed in Great Britain. All rights reserved
0032-3861/96/$15.00 + 0.00

Fusion bonding of maleic anhydride grafted polypropylene to polyamide 6 via *in situ* block copolymer formation at the interface

Jacques-Eric Bidaux, Gregory D. Smith, Nicolas Bernet and Jan-Anders E. Månson*
Laboratoire de Technologie des Composites et Polymères, Ecole Polytechnique Fédérale de Lausanne, CH-1015 Lausanne, Switzerland

and Jöns Hilborn
Laboratoire des Polymères, Ecole Polytechnique Fédérale de Lausanne, CH-1015 Lausanne, Switzerland

(Received 9 May 1995; revised 31 July 1995)

Bond formation between maleic anhydride-*g*-polypropylene (PPg) and polyamide 6 (PA) by *in situ* block copolymer formation has been investigated. The effects of bonding temperature and time on the critical strain energy release rate, G_C, of the bonds were studied. The G_C values were measured using a wedge test in an asymmetric double cantilever beam geometry. Electron spectroscopy for chemical analysis (ESCA) and scanning electron microscopy (SEM) observations of the fracture surfaces were used to provide detailed information on the locus of failure and the failure mechanisms. An increase of G_C with bonding temperature was observed with two well defined transitions corresponding to the melting temperature of PPg and PA. Below the PPg melting temperature, there is no significant adhesion due to the absence of intimate contact between the adherends. Above this temperature, G_C increases gradually with temperature. This is explained by the increased mobility of maleic anhydride grafted PP chains which can migrate towards the interface and react with the amine end-groups of the PA. Optimal bonding, however, requires melting of both polymers and results in the highest G_C values which approach the cohesive G_C of PPg. Analysis of these fracture surfaces via ESCA and SEM have shown that failure was cohesive in the PPg and accompanied by significant plastic deformation. This is interpreted as saturation of the interface by block copolymer due to the mutual migration of the PA and grafted PP polymer chains that becomes possible when the PA melts. It is suggested that as crystallization proceeds each half of the block copolymer is incorporated into crystalline domains on their respective sides of the interface, producing the highest G_C values observed.

(Keywords: fusion bonding; block copolymers; incompatible polymers)

INTRODUCTION

Bonding between different polymers is a key issue for many important technologies; the production of blends, the coextrusion of films and the welding of polymers and composites are examples. The mechanisms through which bonding is achieved are numerous and depend on the nature of the polymers to be joined: compatible or incompatible, semi-crystalline or amorphous. Often, more than one mechanism contributes to the overall adhesion. For amorphous and compatible polymers an adhesive bond forms by the interdiffusion of the molecules across the interface[1–3]. Good adhesion is generally obtained when the molecules diffuse sufficient distance to create entanglements on both sides of the interface. However, if the two polymers are incompatible, mutual interdiffusion is limited and the bond strength is low. For the particular case of incompatible semi-crystalline polymers, significant adhesion can be obtained by the crystallization of one polymer in the presence of a melt of another polymer. At the moment when the spherulites of the crystallizing polymer impinge, the molten polymer will be drawn into the crystallizing polymer. This results in increased interfacial area and, if the volume contraction is localized, in mechanical interlocks known as influxes[4–5]. An interesting alternative, which is applicable for both semi-crystalline and amorphous polymers, is to promote bonding through the use of block copolymers at the interface between the two polymers[6,7]. The simplest type of copolymer is a di-block copolymer where each block is compatible with one of the relevant homopolymers. Investigations of this type have been carried out for amorphous polymers by Creton *et al.*[6], who studied the effect of block copolymer concentration and block molecular weight on adhesion. The addition of block copolymers has been used successfully to improve the mechanical properties of binary blends, where one polymer forms a dispersed second phase in a continuous matrix of the other[8]. The block copolymer improves the

---

* To whom correspondence should be addressed

mechanical properties by reducing the particle size of the dispersed phase and forms a physical link between the dispersed and the continuous phases.

Another approach, studied in the present work, is to form the block copolymer *in situ* when the polymers are brought into contact. This requires chemical reactions at the contacting surfaces and has been used extensively for improving adhesion between polyamide and polyolefins[9–13]. Usually, modified polyolefins containing anhydrides or acids are used. In a recent study of adhesion between polyamide 6 and polypropylene, a polypropylene containing a fraction of tethered succinic anhydride groups which could react with the amine end of polyamide 6 was used[14]. The adhesion strength was studied *versus* time for temperatures below the melting temperature of the polyamide. The results strongly suggested that adhesion occurred by the formation of a copolymer at the interface.

The object of this paper is to investigate the bonding of maleic anhydride grafted polypropylene and polyamide-6. Formation of copolymer is assumed to occur at the interface between the anhydride end-group of the PPg molecule and PA molecule as illustrated in *Figure 1*[15]. In particular, the effect of temperature, varying from below the melting temperature of the polypropylene to above that of the polyamide, on the degree of bonding is studied. The materials were bonded using a technique similar to that developed for studying bonding of polypropylene that has close control over the processing parameters; i.e. temperature and pressure[16]. The goal is to determine the conditions for optimum bonding between two incompatible semi-crystalline materials for application to industrial processes.

EXPERIMENTAL

The materials in this work were polypropylene grafted with 850 ppm maleic anhydride (MAH) containing ethylene-propylene rubber (EPR), grade OREVAC PP-C (PPg), and polyamide-6, grade ORGAMIDE RESNO (PA), both from Elf Atochem S.A. The peak melting temperatures of the PPg and PA were measured using a Perkin-Elmer DSC7 dynamic scanning calorimeter at 20°C min^{-1} and found to be 150 and 221°C, respectively. The flexural moduli were measured at room temperature in three point bending using a Rheometrics RSAII rheometer at 0.016 Hz and found to be 0.52 and 1.67 GPa, respectively.

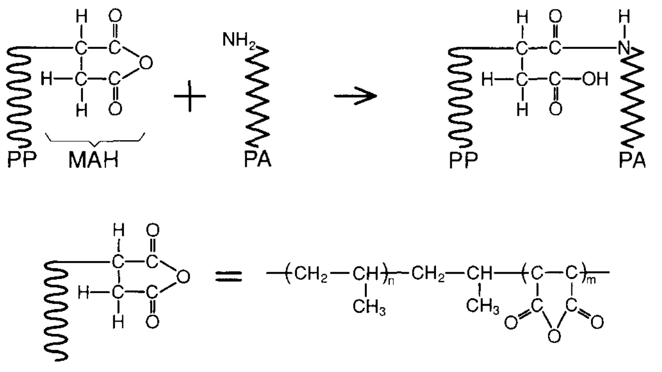

Figure 1 The reaction scheme between MAH-grafted PP and PA (after Ide and Hagesawa[15])

Plaques for the bonding experiments were made on a Butler 10/90 HI-TECH injection moulding unit. The PA granules were dried in a vacuum at 150°C for 18 h before injection. The mould was approximately 50 by 50 by 4 mm deep. Flat steel inserts were laid inside the mould to make 1.3 mm thick PA plaques and 2 and 3 mm thick PP plaques. The melt injection temperature was 225 and 295°C for the PP and PA, respectively. The mould temperature for both materials was 40°C. The pressure cycle was the same for both materials; 60 MPa for the injection phase and 20 MPa for the holding phase. No release agent was used to avoid contamination. The plaques were stored in sealed containers with desiccant.

The bonding experiments were conducted using an instrumented matched-die mould installed on a servo-hydraulic load frame. A schematic of the mould with the heating and cooling systems is shown in *Figure 2*. The temperature was monitored via thermocouples located at the upper and lower moulds. Both mould halves were heated to the same temperature (±1°C) and allowed to equilibrate at temperature for approximately 10 min. A 5 mm wide strip of polyimide (KAPTON) tape, 30 μm thick, was placed on the lower surface adjacent to the polyamide plaque to serve as a crack initiator. Bonds were made by placing both plaques into the mould which was then closed to a pressure of 4 MPa for a specified hold time, at which point the heating was turned off and cooling initiated. The pressure was maintained until the mould reached room temperature.

Two test series were performed: For series 1, the hold time was kept constant at 9 min, while the temperature was varied between 140 and 280°C. For series 2, the temperature was kept constant at 160°C and the hold time varied between 1.25 and 17 min. 10 mm wide strips were cut from the centre of the bonded plaques for use as fracture specimens and the two remaining side pieces saved for optical microscopy examination. A starter crack was initiated in the fracture specimens by aligning a single edged razor blade with the plane of the interface along the Kapton tape and pressed into the specimen. The fracture energy of the bonds were obtained using a double cantilever beam geometry with a constant crack opening displacement as shown in *Figure 3*. Crack

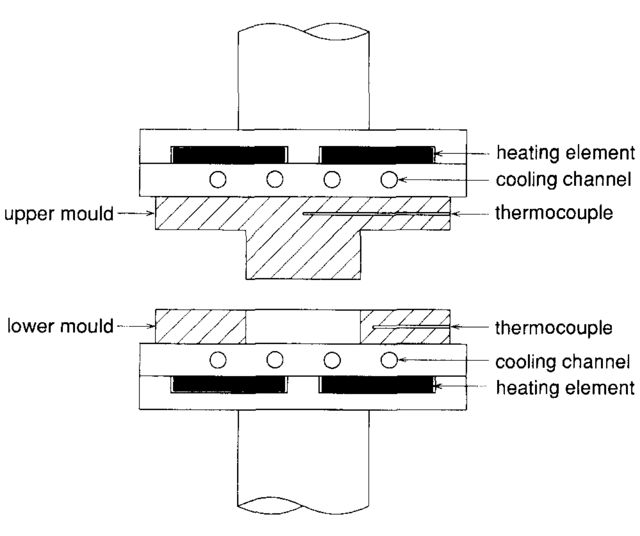

Figure 2 Schematic of the instrumented matched-die mould showing the heating elements and the cooling channels

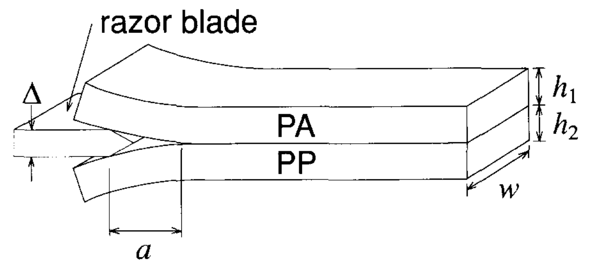

Figure 3 Schematic of the fracture test geometry used to measure the critical strain energy release rate (G_C). A double cantilever beam test with constant crack opening displacement

propagation was accomplished by forcing the specimens over the razor blade in a screw driven load frame at a crosshead speed of $2\,\mathrm{mm\,min^{-1}}$. The crack area was illuminated by placing a lamp behind the specimens and recording the crack area as a function of position from the front using a video camera. Afterwards, the video images were captured and digitized on a personal computer using image analysis software. The crack length was measured at 2.5 mm intervals over a 10 mm length at the mid-point of the specimen. The overall crack length at each position was calculated as the average of 5 crack lengths: 1 at each edge and the other 3 evenly spaced across the specimen width. The crack propagation mode was predominantly stable, but did vary somewhat with position. Occasionally the crack front would reach an area of poor bonding and jump 1 to 2 mm, stopping at the next area of higher toughness and grow as before. Only data from stable crack growth have been reported.

After recording the crack lengths, the bonded specimens were split in half and the fracture surfaces examined using ESCA to determine their chemical composition. Fracture surfaces were also coated with a thin layer, approximately 30 nm thick, of Au-Pd and examined in a SEM (JEOL JSM-6300F).

Optical microscopy was used to characterize the cross-sectional morphology of the interface. Microtomed sections, approximately 10 μm thick, were cut perpendicular to the plane of the interface from the edge of the remaining side pieces directly adjacent to the fracture specimen. The central portion of these sections were then viewed between crossed polarizers.

DATA ANALYSIS

The critical strain energy release rate was calculated using an equation derived by Kanninen[17] based on the bending of a prismatic beam supported by an elastic foundation. The key assumptions for this equation are (i) the only contribution to the stored elastic energy of the system is from the bending of the free portions of the beams and the elastic deformation ahead of the crack tip, (ii) the elastic energy stored ahead of the crack tip is well described by an elastic foundation and (iii) all the elastic energy released upon fracture is absorbed by plastic deformation at the crack tip[7]. For this case G_C is given by

$$G_C = \frac{3\Delta^2 E_1 h_1^3 E_2 h_2^3}{8a^4}\left(\frac{E_1 h_1^3 C_2^2 + E_2 h_2^3 C_1^2}{(E_1 h_1^3 C_2^3 + E_2 h_2^3 C_1^3)^2}\right) \tag{1}$$

with $C_1 = 1 + 0.64\ h_1/a$, $C_2 = 1 + 0.64\ h_2/a$, where Δ is the wedge thickness, E is the elastic modulus, h is the beam thickness, a is the crack length and the subscripts 1 and 2 refer to PA and PPg, respectively. Equation (1) is only valid if the crack propagation occurs along the bimaterial interface. According to Xiao *et al.*[18], for a symmetric double cantilever beam geometry using materials with different elastic moduli, there is a K_{II} component in the stress intensity factor near the crack tip which causes the crack to grow into the more compliant material, in our case the PPg. To avoid this, an asymmetric geometry using h_2/h_1 ratios of 1.5 and 2.3 were used to force the crack to follow the interface. Equation (1) was also used for calculating the mode I G_C values of bulk and bonded PPg specimens.

Computation of the fracture toughness from equation (1) requires knowledge of the elastic moduli E_1 and E_2 of each material. Since the elastic moduli are time and frequency dependent, it is important to determine the time scale Δt over which stress is applied to a volume element during crack propagation[19]. This is a complex task, since during a crack propagation experiment each volume element experiences a complex, time dependent, history with a variable strain rate. Nevertheless, as a first approximation, Δt can be taken as the time during which a volume element, initially at the crack tip, remains located between the crack tip and the wedge and thus undergoes bending. This is the time available for relaxation and is given by

$$\Delta t = a/\dot{a} \tag{2}$$

where a is the crack length and $\dot{a}$ is the crack propagation velocity. Accordingly, G_C was computed using the elastic moduli measured dynamically at a frequency ν given by

$$\nu = 1/\Delta t = \dot{a}/a \tag{3}$$

For the crack velocities used in our experiments, this frequency is of the order of 0.01 Hz.

RESULTS

Interfacial fracture energies

The fracture energies for the first series of experiments as a function of the temperature are shown in *Figure 4*. The overall trend is increasing fracture energy with bonding temperature. Furthermore, this increase occurs in three distinct temperature regions: (i) a region below the melting temperature of PPg where there is virtually no adhesion (no specimens survived the preparation procedures for wedge testing), (ii) a region between the melting temperatures of PPg and PA where the fracture energy increases with temperature, and (iii) a region above the melting temperature of PA where the fracture energy is essentially constant. It can be seen that there is essentially no influence of the degree of asymmetry on the values of G_C for the h_2/h_1 ratio used in region (i) and (ii). In region (iii), no valid results were obtained for the h_2/h_1 ratio of 1.5 due to failure in bending of the PPg adherend at the crack tip.

In region (i) both materials are solid and one would not expect any bonding to occur. The fact that the plaques stuck together until destroyed by further specimen preparation may be due to the fact that at 140°C approximately 40% of the PPg which was initially crystalline had melted (according to d.s.c. data). Thus it may be possible that this partially molten material can

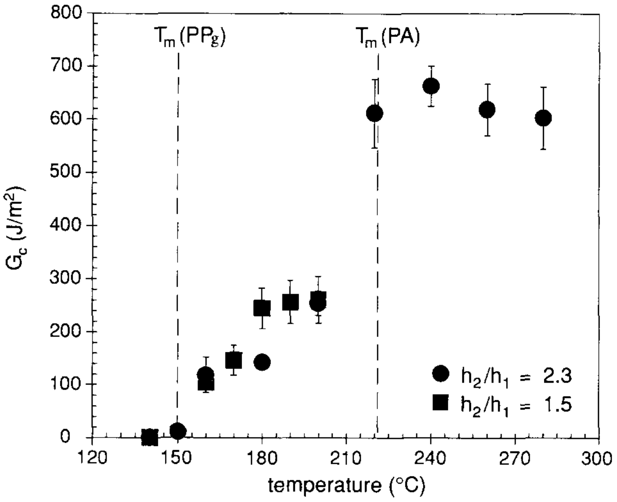

Figure 4 The critical strain energy release rate (G_C) as a function of temperature. T_m(PPg): melting temperature of PPg. T_m(PA): melting temperature of PA

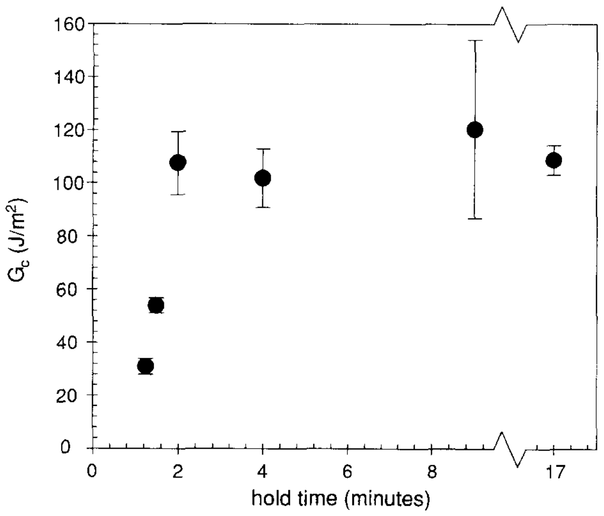

Figure 5 The critical strain energy release rate as a function of hold time at a bonding temperature of 160°C

interact with the PA, although there could only be a very weak interaction, since the presence of the remaining crystalline domains will greatly reduce any molecular mobility.

In region (ii) there is a steady increase in the G_C values. In this region the PPg is completely molten and the polymer chains are now able to diffuse. The MAH end-group of the PP is polar and may diffuse to the interface region and concentrate on the higher energy PA surface. The driving force for the migration of MAH segments to the interface is the reduction in surface energy. The migration may occur by phase separation, diffusion and surface adsorption[3]. The MAH graft may react with the amine group in the amorphous regions at the PA interface, explaining the observed increase in adhesion.

In region (iii) the highest values for G_C are obtained. This is not surprising since both the PPg and the PA are molten and thus, interaction between the MAH and the PA becomes highly probable. The mobility of polyamide amine end-groups increases dramatically. Diffusion may occur over longer distances and anhydrides react with amine groups to saturate the interface with block copolymer and improve the adhesion.

Two additional reference experiments were carried out. In the first experiment, the wedge was driven through a single, 3 mm thick, PPg plaque where a starter crack was initiated as previously described and gave $G_C = 790 \pm 80$ (J m^{-2}). This value represents the fracture energy for cohesive failure in PPg. In the second experiment, the G_C value for two PPg plaques, bonded at 180°C with a hold time of 9 min, gave a G_C value of $G_C = 830 \pm 40$ (J m^{-2}). The close agreement between these two values suggests that the processing conditions for the second experiment produce a completely healed interface. Comparing these values to those of region (iii) shows that the region (iii) bonds are indeed strong and are close to those corresponding to cohesive failure in PPg. It may be surprising to obtain such a strong bond, even at temperatures above 250°C, since oxidative degradation of PPg already occurs at 215°C from our d.s.c. experiments. The absence of a significant degradation in the bonding experiments is probably a result of the protection by the closed mould.

The effect of hold time on fracture energy for bonds made at 160°C is shown in *Figure 5*. This temperature was chosen to be above the PPg melting temperature to obtain sufficient adhesion, but as low as possible to reduce the reaction rate and make it detectable within the time frame of the experiment. Initially, the fracture energy increases very quickly, essentially linearly, with hold time, but it then levels off to a constant value at approximately 2 min. The initial increase is expected since the more time that is available for diffusion, the higher the number of reactions between the MAH and the PA. The fast increase in G_C and its abrupt levelling off suggests that the diffusion and reaction process is quite fast at this temperature, and that the interface becomes saturated by MAH-grafted chains. The increase in fracture energy does not follow the $t^{1/2}$ law predicted by reptation theory[1]. It is clear, however, that a more extensive study including the influence of temperature is needed.

Fracture surface morphology

Shown in *Figure 6* are the fracture surfaces of the PA side of the specimen from each region. *Figure 6a* shows the fracture surface from region (i). The most visible features of this micrograph are the horizontal lines which, after a comparison with an as-moulded plaque, were determined to be the ground surface texture of the moulds from the injection moulding operation. The fracture surface of a bond made in region (ii) is shown in *Figure 6b*. The as-moulded surface texture is still visible, but it is obscured by ridges of material which form irregular polygons. The average spacing between these ridges is approximately 3 μm. The fracture surface for a bond made in region (iii) is shown in *Figure 6c*. Since both the PPg and PA are molten, one would not expect to observe any of the as-mould surface texture and, indeed, none is seen. The most significant feature is the scale of the deformation which is much larger than in region (ii) and has correspondingly higher fracture energies. Strong plastic deformation is clearly visible with fibril formation. Since plastic deformation is a highly energy dissipative mechanism, it accounts for the

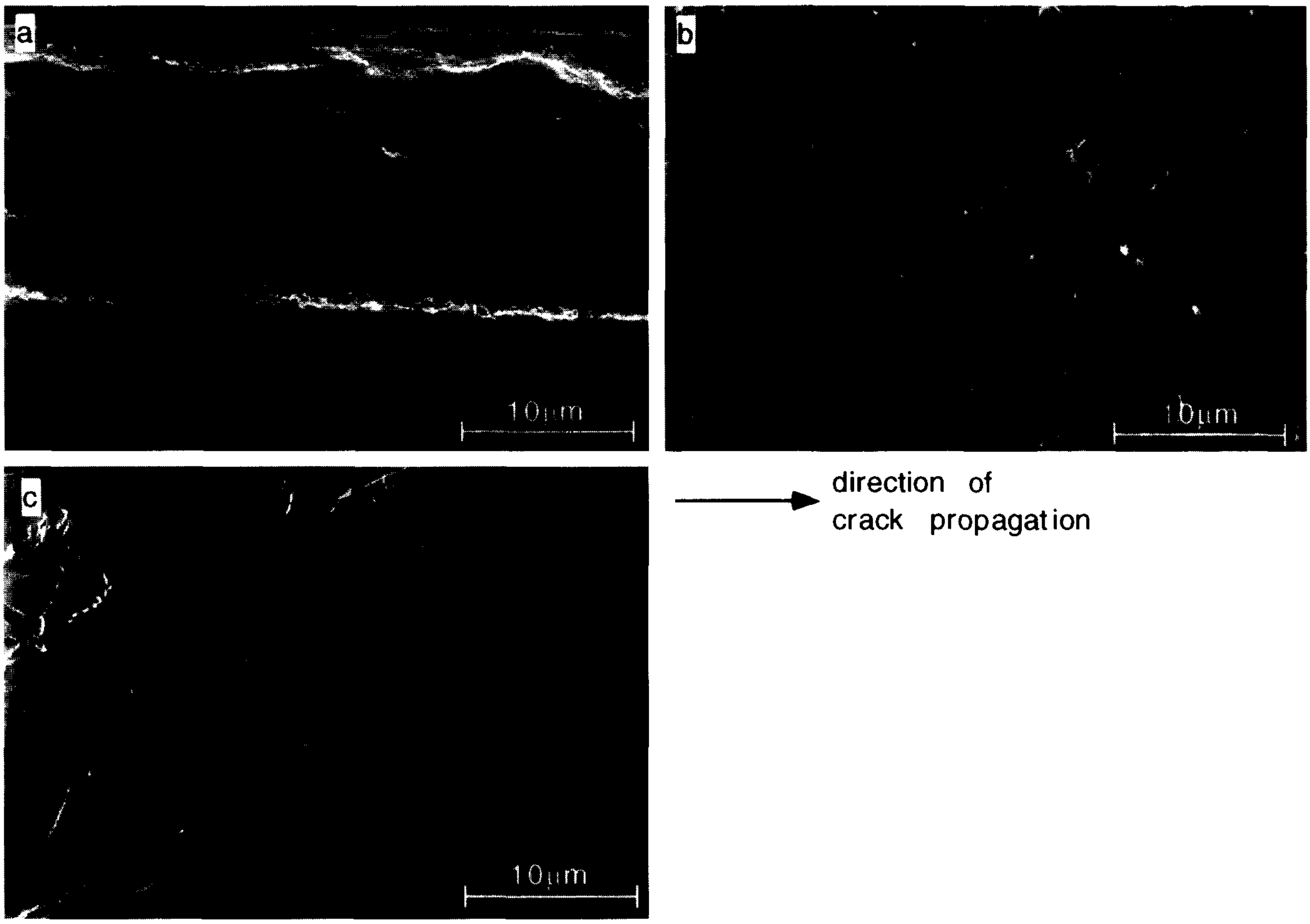

Figure 6 Scanning electron micrographs of the fracture surface morphology of the PA for different bonding temperatures: (a) 140°C; (b) 160°C; (c) 240°C

increase in fracture energy observed between region (ii) and region (iii).

Cross-sectional morphology

The cross-sectional morphologies for two bonds of the first series are compared in *Figure 7*. *Figure 7a* shows the bond made at 180°C. The PA is essentially unchanged from the as-moulded condition with an approximately 60 μm layer of amorphous material directly adjacent to the bond interface. In the PPg side of the bond there are essentially equiaxed spherulites. Inspection of the PPg material directly adjacent to the interface at higher magnification produced an estimate of 6 μm for the average spherulite diameter. (This estimation is quite difficult to make since the presence of the maleic anhydride end-groups and EPR reduces the crystallinity to only 20%, measured via d.s.c., and results in poorly defined spherulite boundaries.) *Figure 7b* is the cross-section for the bond made at 260°C. The key difference between *Figure 7b* and *7a* is the absence of the amorphous layer in the PA. Since both materials are molten and cooled reasonably slowly, the PA can crystallize into more and larger spherulites than was possible during cooling in the injection mould, resulting in the spherulites with easily distinguished boundaries. The measured average diameter of 3 μm for the irregular polygons from the PA fracture surfaces at 160°C compares reasonably well with the 6 μm measured spherulite diameter from the cross-sectional morphology of the 180°C bond. The larger average diameter for the 180°C bond is expected since, at a higher temperature the material will have a longer time to crystallize, thus producing large spherulites. This agreement suggests that the source of the ridges of material visible in *Figure 6b* could be the result of amorphous material being concentrated at the spherulite boundaries. The polypropylene chains containing a MAH graft will have a lower molecular weight (the MAH end-groups bond to the polypropylene chain by scission, thus lowering the molecular weight of the chain to which it is attached). The relatively bulky MAH end-groups are not easily accommodated into the crystalline lamellae; therefore, they may be rejected from the growing lamellae, tending to concentrate in the regions between adjacent lamellae and at spherulite boundaries, producing the observed ridges. The ridges may also be due to the easily deformable amorphous EPR rubber inclusions, but these are not likely to adhere strongly to the PA, although one would expect the EPR to enhance fracture energy dissipation.

Chemical surface analysis

To determine if the fracture was adhesive or cohesive, the chemical composition of the fracture surfaces were analysed by ESCA for three bonding temperatures. The elemental composition of the reference (as-moulded) PA and PPg plaques and the fracture surfaces shown in *Figure 6* are given in *Table 1* and represent the average

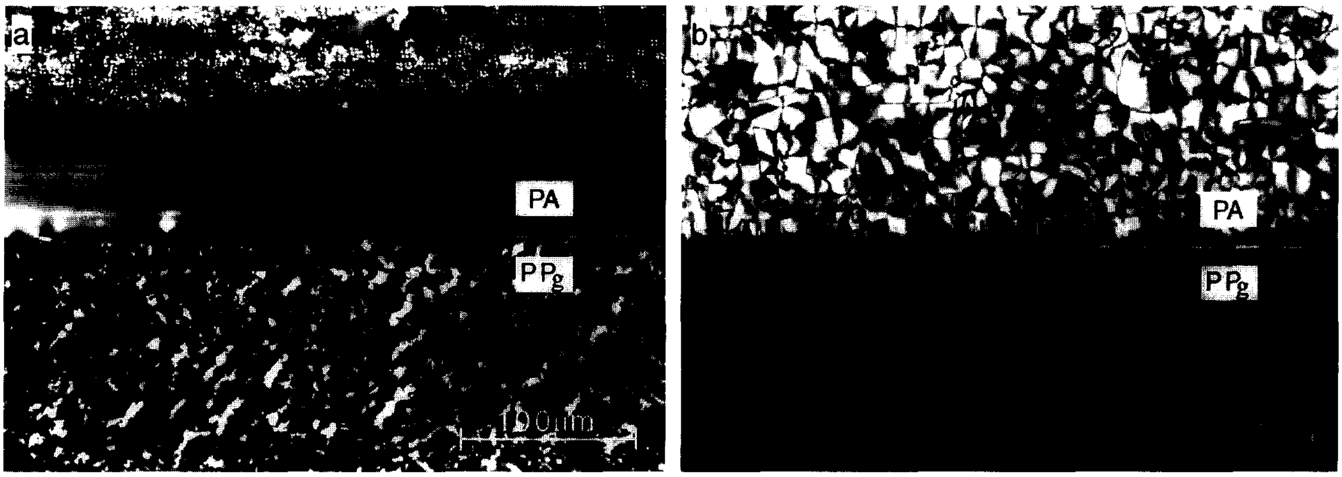

Figure 7 Cross-sectional morphology for bonds made at (a) 180°C and (b) 260°C, i.e. below and above the melting temperature of PA

compositions taken over the area of the electron beam (0.5 mm in diameter). The elemental composition of the reference PA has the expected ratio between oxygen and nitrogen, but gives a somewhat higher than expected value for carbon. As expected, no nitrogen was detected for the reference PPg, however, due to the MAH graft, oxygen was detected. At 160°C, the PA fracture surface shows a decrease in oxygen and nitrogen concentrations and an increase in carbon concentration indicating that the PA surface is covered either by a layer of PPg (less than 50 Å thick, so that the PA signal can still be detected) or by patches of PPg with PA still visible between them. Comparison with the associated fracture surface morphology (*Figure 6b*) suggests that, in this temperature range, failure occurs in the PPg, but very close to the PA surface. As the bonding temperature is increased, the difference between the surface compositions disappears and becomes identical to the PPg signal. Thus for the 180 and 200°C bonding temperatures, the PA side of the specimens is completely covered by a layer of PPg. The surface texture of the mould is no longer visible indicating that the thickness of the PPg layer is greater than the 1 μm roughness of the PA surface. However, from optical microscopy observations the crack appears to be propagating along the interface, suggesting that the layer thickness is on the order of several microns.

DISCUSSION

The absence of any significant adhesion at temperatures lower than 160°C indicates that the melting of at least one of the adherends, PPg in this case, is a necessary condition to produce the intimate contact and chain mobility needed for adhesion. This is consistent with a related study by Bothe and Rehage[4] on autohesion of crystalline elastomers. In highly crystalline materials a large number of chain ends are immobile because they are trapped in crystalline domains. Adhesion can only be effected by raising the temperature above the melting range of the polymer or by solvating the contact surfaces by a suitable solvent.

Table 1 Elemental compositions of fracture bond surfaces as measured by ESCA. Concentrations in atomic percent

T_{bonding} (°C)	PA C	PA O	PA N	PPg C	PPg O	PPg N
reference	86	7	7	98	2	0
160	97	2	1	99	1	0
180	99	1	0	99	1	0
200	97	3	0	97	3	0

Above the melting point of PPg (about 160°C), flow and mobility are sufficient for the grafted PP chains to achieve intimate contact and react with the PA chain ends to produce PP-MAH-PA block copolymers at the interface. The copolymers serve as a primary bond between the two polymers which is seen as an increase in adhesion. The onset of interfacial reactions is reflected in the ESCA results: the fracture surfaces of the 180 and 200°C bonds exhibit compositions very much resembling PP, suggesting the presence of PP strongly attached to the PA surface. Upon adhesive failure, the linking copolymers at the interface give rise to a limited fracture energy due to the pull-out of the PP portion of the block copolymer combined with detachment of PP patches from low strength, possibly amorphous PP areas. The fact that the mould texture is still visible indicates that failure occurred within the PPg, but very close to the interface. This is probably due to the existence, at the PA/PPg interface, of a thin interphase with a high concentration of low molecular weight grafted chains. These low molecular weight chains can migrate easily and gives rise to interface enrichment. An interphase formed of such low molecular weight chains has relatively low cohesion and, therefore, the crack tends to propagate through this zone[20,21].

Upon raising the bonding temperature to 180°C, the molecular mobility increases slightly and hence, the amount of interfacial reactions that produce block copolymers also increases. The amount of chains that have to be pulled out at fracture increases slightly resulting in more detached PPg and a small increase in G_C. The amount of PPg residing on the PA side after fracture is now large enough to cover the surface completely, as seen from the ESCA results.

When the bonding temperature is above the crystalline melting point of PA, not only the grafted PP chains, but also the PA chains are mobile. A larger number of

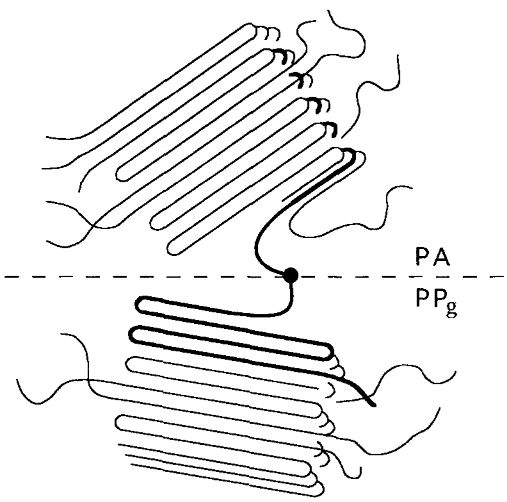

Figure 8 A schematic of the block copolymer linked on both sides into crystalline domains and acting as a tie molecules over the interface

reactions is possible, which leads to the saturation of the interface with block copolymer. The dramatic increase in failure energy is accompanied by a change of failure mode and deformation mechanism. The fracture occurs cohesively in the PPg, but is still relatively close to the interface. From the micrograph of the fracture surface in *Figure 6c*, large ductile deformation is visible with fibril formation. It is clear that the deformation involves crystalline domains in the PPg giving rise to the significant improvement in failure energy. It may be that the excellent adhesion comes from the incorporation of each copolymer block into the crystalline domains formed on both sides of the interface during subsequent cooling from the bonding temperature. The block copolymers are linked on both sides into crystalline domains and can act as tie molecules across the interface, as shown schematically in *Figure 8*. The interfacial adhesion is now sufficient to plastically deform the PP crystalline domains which results in substantially improved energy dissipation. The onset of chemical reactions may best explain the observed increase in fracture energy, however there may be a small contribution from influxes. Indeed the interface corresponding to the bonds made above the melting point of PA (*Figure 7b*) is more sinuous and presents a higher surface area than the one associated with a bond formed below the PA melting point (*Figure 7a*). In addition, a non-planar interface may also be energetically more favourable when the concentration of block copolymers becomes very high. This aspect is currently being studied in more detail.

CONCLUSIONS

The fracture energy, G_C, of fusion bonded PPg/PA interfaces is strongly dependent on the bonding temperature. The fracture energy increases with bonding temperature, with two well defined transitions corresponding to the melting temperature of each material.

Below the PPg melting temperature, virtually no adhesion is observed. Melting of PPg gives rise to a significant improvement of the bond fracture energy. Between the PPg and PA melting temperatures, G_C increases with increasing bonding temperature. Failure occurs in PPg, within a thin interphase of low cohesion close to the PA surface. Melting of PPg achieves intimate contact between the adherends and increases the mobility of the PP chains. Migration of MAH-grafted PP chains towards the interface occurs and leads to copolymer formation by chemical reaction with PA amine end-groups resulting in improved fracture energy.

Optimal bonding of PPg to PA requires the melting of both adherends. For bonding temperatures exceeding the melting temperature of PA, values of fracture energy close to the cohesive fracture energy of PPg are observed. The fracture surfaces show cohesive failure in the PPg with significant plastic deformation. In this temperature range, not only are the PP chains mobile, but so are the amine end-groups. The amine end-groups can migrate towards, and saturate, the interface with copolymers which now act as tie molecules between the two polymers. It is hypothesized that as crystallization proceeds, each block of the copolymer is incorporated into crystalline domains on both sides of the interface, producing maximum adhesion.

ACKNOWLEDGEMENTS

Critical reading of the manuscript by Professor H. H. Kausch and Dr D. Knauss is gratefully acknowledged. We also thank N. Xanthopoulos and Professor H. J. Mathieu from Laboratoire de Métallurgie Chimique of Ecole Polytechnique Féderale de Lausanne for the help in performing the ESCA measurements and B. Senior from Centre Interdépartemental de Microscopie Electronique of Ecole Polytechnique Féderale de Lausanne for the scanning electron microscopy. Financial support of this work was provided by the Priority Program for Materials (PPM) in Switzerland.

REFERENCES

1 Jud, K., Kausch, H.-H. and Williams, J. G. *J. Mater. Sci.* 1981, **16**, 204
2 Brown, H. R. *Ann. Rev. Mater. Sci.* 1991, **21**, 463
3 Bothe, L. and Rehage, G. *Rubber Chem. Technol.* 1981, **55**, 1308
4 Yuan, B.-L. and Wool, R. P. *Polym. Eng. Sci.* 1990, **30**, 1454
5 Bartczak, C. and Galeski, A. *Polymer* 1986, **27**, 544
6 Creton, C. Kramer, E. J., Hui, C.-Y. and Brown, H. R. *Macromolecules* 1992, **25**, 3075
7 Cho, K., Brown, H. R. and Miller, D. C. *J. Polym. Sci. B: Polym. Phys.* 1990, **28**, 1699
8 Chen, C. C., Fontan, E., Min, K. and White, J. L. *Polym. Eng. Sci.* 1988, **28**, 69
9 Duvall, J., Sellitti, C., Myers, C., Hilter, A. and Baer, E. *J. Appl. Polym. Sci.* 1994, **52**, 195
10 Duvall, J., Sellitti, C., Myers, C., Hilter, A. and Baer, E. *J. Appl. Polym. Sci.* 1994, **52**, 207
11 Duvall, J., Sellitti, C., Topolkaraev, V. Hilter, A., Baer, E. and Myers, C. *Polymer* 1994, **35**, 3948
12 Nishio, T., Suzuki, Y., Kojima, K. and Kakugo, M. *J. Polym. Eng.* 1991, **19**, 123
13 Lee, Y. and Char, K. *Macromolecules* 1994, **27**, 2603
14 Boucher, E., Folkers, J. P., Hervet, H. and Leger, L. *Proc. Eur. Conf. on Adhesion*, Mulhouse, 1994, p. 442
15 Ide, F. and Hasegawa, A. *J. Appl. Polym. Sci.* 1974, **18**, 963
16 Smith, G. D., Toll, S. and Månson, J.-A. E. *Proc. 3rd Int. Conf.*

on Flow Processes in Composite Materials, Galway, Ireland, 7–9 July, 1994, p. 423
17 Kanninen, M. F. *Int. J. Fract.* 1973, **9,** 83
18 Xiao, F. Hui, C.-Y. and Kramer, E. J. *J. Mater. Sci.* 1993, **28,** 5620
19 de Gennes, P. G. *C. R. Acad. Sci. Paris* 1988, **307,** Série II, 1949
20 Schulz, J. *J. Adhesion* 1992, **37,** 73
21 Schulz, J., Lavielle, L., Carre, A. and Comien, P. *J. Mater. Sci.* 1989, **24,** 4363